DOI: 10.1002/anie.200804339

Expanded Metals

Structure and Phase Behavior of the Expanded-Metal Compound $^7Li(ND_3)_4$**

Richard M. Ibberson, Amelia J. Fowkes, Matthew J. Rosseinsky, William I. F. David, and Peter P. Edwards*

Ammonia is a unique solvent that dissolves all the alkali metals, the alkaline-earth metals (Ca, Sr, and Ba), and the lanthanide metals (Eu and Yb).[1] The alkali metal lithium, the alkaline-earth metals calcium, strontium, and barium, and the rare-earth elements europium and ytterbium all form compounds of the type $Li(NH_3)_4$ and $Ca(NH_3)_6$ that are best viewed as expanded metals,[2] in which the metal atoms are spatially separated by the diluent (i.e. dielectric ammonia). Lithium(0)tetraamine, $Li(NH_3)_4$, is the lightest metallic solid, which is golden-bronze in color, a metallic conductor, and has the lowest melting point[3,4] (−184 °C) of any metal. It has unusual electrical[5] and magnetic[6–8] properties that include the appearance of localized moments and apparent subsequent antiferromagnetic coupling. Ab initio calculations[9] show that the valence electrons in the molecules are expanded considerably in relation to the 2s function of atomic lithium giving rise to a Rydberg-like ground state. Electron densities in metals are often characterized by the linear measure r_s, defined for a volume containing n free electrons by $(4/3\pi n)^{-1/3}/a_o$, where a_o is the effective Bohr radius. Typical values of r_s for all of the metallic elements are in the range of 2–5.6 with the highest value found for the cesium atom. Remarkably, the r_s value for $Li(NH_3)_4$ is 7.4, raising the intriguing possibility of strong electron–electron interactions for a compound which appears to lie just to the metallic side of the Mott (metal–insulator) transition.

There are numerous practical difficulties associated with experimental studies of lithium(0)tetraamine, and reliable structural information is elusive. A re-evaluation[10] of early powder X-ray[11] and neutron diffraction[12] experiments coupled with electrical, magnetic, and thermal data concluded that lithium(0)tetraamine has three stable forms with body-centered cubic (bcc) structures based on the packing of distinct $Li(NH_3)_4$ complexes. Phase I is stable between the melting point and 82 K ($a = 14.98$ Å at 85 K) and is most likely an orientationally disordered plastic phase. Phase II is stable between 82 K and approximately 25 K ($a = 14.93$ Å at 60 K), with probable space group $I\bar{4}3d$. The phase III structure below 25 K ($a = 14.80$ Å at 20 K) gives rise to weak superstructure reflections corresponding to a doubling of the cubic lattice parameter and associated with possible antiferromagnetic coupling. There are very strong isotope effects that are most pronounced in the observation of three phases in $Li(NH_3)_4$ and only two in $Li(ND_3)_4$.[4] No phase change at 82 K is observed for $Li(ND_3)_4$, suggesting that this transition becomes associated with the onset of melting. The most recent and reliable structure of phase II of $Li(ND_3)_4$ has been determined by neutron powder diffraction[13] and confirms the idealized crystal structure proposed earlier,[10] although also indicating strong distortions to the pyramidal structure of each molecular complex. A detailed evaluation of the low-temperature structures of lithium(0)tetraamine remains an important and unsolved problem in metal–ammonia chemistry, despite a long history of investigations, and is the motivation for the present studies.

The refined cubic lattice constants for $^7Li(ND_3)_4$ determined by high-resolution neutron powder diffraction studies are shown in Figure 1 and are in agreement with the reported data.[10] The lattice constant shows a smooth variation with temperature, and no obvious anomaly is observed corresponding to the phase transition from phase II to phase III. However, supercell peaks, as noted previously[3] corresponding to a possible doubling of the cubic lattice parameter, were observed in the range between 4.2 and 22 K. The experimental data were fitted using Einstein and Debye functions that are more typically associated with the analysis of heat capacity data. An excellent fit can be obtained using a

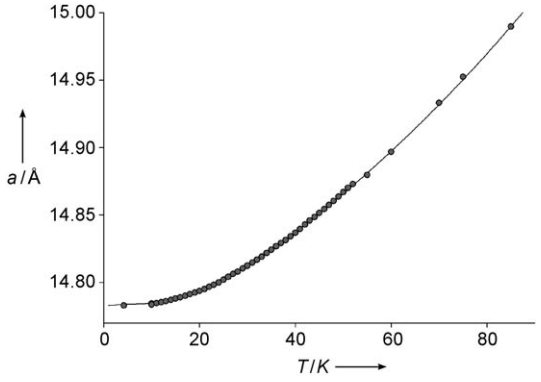

Figure 1. Variation of the cubic lattice parameter a of $^7Li(ND_3)_4$ as a function of temperature. The data are fitted using an Einstein plus Debye model (see main text).

[*] Dr. R. M. Ibberson, Prof. W. I. F. David
ISIS Facility, STFC-Rutherford Appleton Laboratory
Harwell Science and Innovation Campus
Didcot, Oxfordshire, OX11 0QX (UK)
E-mail: r.m.ibberson@rl.ac.uk
Dr. A. J. Fowkes, Prof. M. J. Rosseinsky,[+] Prof. P. P. Edwards
Inorganic Chemistry Laboratory, University of Oxford
South Parks Road, Oxford OX1 3QR (UK)
[+] Present address: Department of Chemistry, University of Liverpool
Liverpool, L69 7ZD (UK)

[**] We thank STFC for the provision of neutron beam time.
Supporting information for this article is available on the WWW under http://dx.doi.org/10.1002/anie.200804339.

single-Einstein plus single-Debye model with values for the refined temperatures of 58.24(3) and 565.8(1) K, respectively, and a value of 14.7823(1) Å for the lattice constant at 0 K. The refined characteristic temperatures correspond to vibrational wavenumbers of 40 and 393 cm^{-1}, values that could represent in each case an average over the lattice modes and molecular modes, respectively, although there are no corroborative vibrational spectroscopy data available for either isotopologue.

The high quality of the neutron powder diffraction data obtained in the current study (Figure 3), in particular at high Q ($Q = 2\pi/d$, where d is the spacing between lattice planes), is crucial to enable an accurate and precise structure determination of lithium(0)tetraamine. Crystallographic parameters are summarized in Table 1. In the phase II structure at 40 K, the molecular complex adopts a near ideal geometry (Figure 2) with only a small (0.043 Å) and barely significant discrepancy between the Li–N1 and Li–N2 bond lengths determined as 2.035(5) Å and 2.078(5) Å, respectively. Similarly the intramolecular geometry of the amine groups freely refines to near ideal values. Refinement of the phase II data at 75 K shows a very similar structural description. By contrast, in the previous neutron powder diffraction study[13] the complex was found to exhibit a strongly distorted pyramidal shape with an apical Li–N1 bond length of 2.488(16) Å and three equivalent basal plane Li–N2 bond lengths of 1.984(4) Å, a difference of 0.504 Å. This earlier observation led to the suggestion that the complex may be better described by the formula $Li(ND_3)_3{\cdot}ND_3$ with the weakly bound ND_3 group perhaps having the tendency to reorient or even dissociate with respect to the complex and so explain the phase I–phase II transition observed for the protonated complexes. The improved data quality of our present study now rules out this highly distorted intracomplex geometry. Indeed the newly refined molecular geometry now supports both ab initio calculations of lithium–ammonia clusters suggesting a Li–N bond length of 2.05 and 2.09 Å[14] depending on details of the model used and also ab initio calculations for the molecular crystal[9] that derive a Li–N bond length of 1.89(2) Å and N–H bond length of 1.03(2) Å. The nature of the conduction states calculated in the ab initio calculations for the molecular crystal prompted the suggestion that $Li(ND_3)_4$ may be an example of a 3D metallic electride.[15,16]

Table 1: Crystallographic data for $Li(ND_3)_4$.

	Phase III	Phase II	Phase II
space group	$P2_13$ (198)	$I\bar{4}3d$ (220)	$I\bar{4}3d$ (220)
T [K]	10	40	75
a [Å]	14.78342(1)	14.83692(2)	14.95223(3)
V [Å^3]	3230.91(1)	3266.02(1)	3342.86(1)
Z	16	16	16
ρ_{calcd} [g cm^{-3}]	0.716	0.709	0.692
R_p	0.0178	0.0214	0.0215
R_{wP}	0.0232	0.0276	0.0273
R_E	0.0118	0.0162	0.0193
GoF	1.97	1.71	1.41

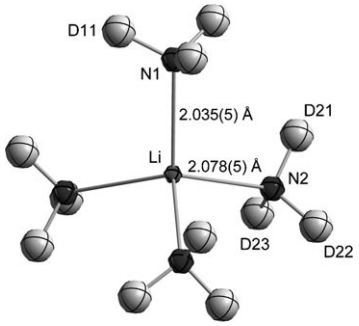

Figure 2. $Li(ND_3)_4$-II at 40 K with isotropic displacement parameters set at 50% probability. Selected bond lengths [Å]: N1–D11 1.013(3); N2–D21 0.992(3); N2–D22 0.972(3); N2–D23 0.994(3). Selected bond angles [°]: N1-Li-N2 109.9(2); N2-Li-N2 109.0(2).

Observation of the phase III structure was first noted following low-resolution constant wavelength neutron powder diffraction experiments.[12] Data recorded at 3 K showed several additional peaks that disappeared above 30 K and these findings were supported by low-temperature differential thermal analysis measurements, which detected a thermal anomaly on both cooling and warming at 27 ± 5 K. Subsequent re-evaluation of these diffraction data successfully indexed the observed additional peaks using a bcc lattice, as in phase II, but with a superstructure of period $2a$.[10] This interpretation is consistent with, and perhaps influenced by, magnetic susceptibility measurements suggesting that phase III may be antiferromagnetically ordered.[7] One anomaly noted in this analysis, however, was that it failed to account for the lowest-angle line observed in the powder diffraction data. The reflection was very weak and not observed in all detectors but corresponds to the (110) reflection that is systematically absent in a bcc lattice.

Analysis of the present high-resolution neutron data for phase III at 10 K shows that the patterns can be readily indexed using the a lattice constant of phase II, whilst adopting a simple cubic (sc) structure and thus a primitive rather than body-centered lattice (Figure 3). The transforma-

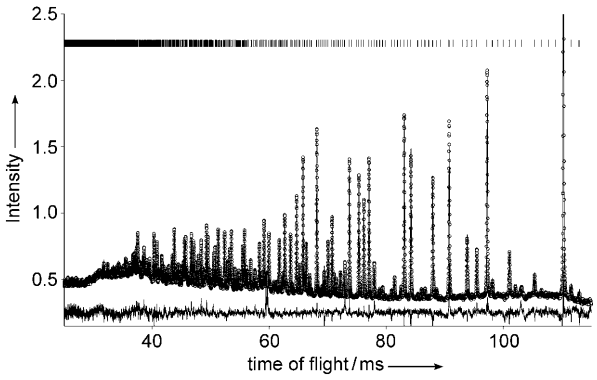

Figure 3. Final Rietveld refinement plot of $Li(ND_3)_4$-III at 10 K, showing observed (○), calculated (line), and difference (lower) profiles. Vertical bar markers indicate calculated Bragg peak positions. The equivalent d spacing range corresponds to 0.75–2.3 Å.

tion from phase II to phase III therefore involves only very small changes in the displacements and orientations of the molecular complexes. There are four independent molecules in the asymmetric unit of phase III and in an initial idealized model of the phase III structure, the refined displacement and anti-displacement parameter of the lithium atoms is only 0.053(2) Å from the starting positions based on the phase II structure. In the final unconstrained refinement, the maximum displacement associated with the Li4 atom is 0.105(5) Å. All four molecules in the asymmetric unit essentially retain the ideal tetrahedral intramolecular geometry observed in the phase II structure. The average Li–N bond for all molecules is 2.08 Å with a root-mean-square deviation of 0.09 Å. The largest structural distortions are associated with the movement of individual molecules along the [111] direction. In phase II the Li···Li intermolecular separation is 6.425(6) Å. In phase III the attendant displacements of the molecules along the [111] direction results in a spread of Li···Li separations of between 6.202(9) Å and 6.729(9) Å. These changes in the crystal packing are reflected in the larger spread of distances observed for the [111]-aligned Li–N bonds. The intermolecular interactions for both structures are dominated by D···D contacts. In phase II the shortest contact distance is 2.857(4) Å, whereas this cut-off distance drops to 2.775(9) Å in the denser phase III structure.

The success in fitting the 10 K phase III diffraction profiles with a model consisting solely of nuclear scattering is significant with regard to the nature of magnetism or electronic coupling in these complexes. It should be emphasized that the superstructure peaks associated with the phase III transition are observed down to short, sub-Ångstrom d spacings, corresponding to Q values in excess of 7 $Å^{-1}$ (Figure 4). Furthermore, the intensities of these peaks remain consistent across all the recorded diffraction data, which extends to lower Q values of circa 1 $Å^{-1}$. Consideration of magnetic form factor fall-off precludes that these peaks are due to magnetic scattering. For example, conventional antiferromagnetic ordering of a typical 3d transition metal would show a drop in intensity of some 90% over this Q range.

The available susceptibility measurements[6,7] do not give strong evidence to support conventional antiferromagnetism occurring in either $Li(NH_3)_4$ or in the deuterated isotopologue. In each case, the maximum in the susceptibility curve is both broad and not very pronounced. The possibility of a transition to a spin density wave below circa 25 K has been proposed,[17] in which case the low-temperature ground state is some form of magnetically ordered expanded metal. Given the low electron density of the metal in this case, it is the correlations between the conduction electrons, which give rise to any antiparallel spin alignment producing periodic spin density. Therefore the ordered moment per lithium atom would as a consequence be very small, and much less than $S = 1/2$ for a theoretically fully localized moment. Such a model is consistent with the present neutron diffraction studies, but only insofar that any neutron magnetic scattering would be necessarily very weak and with a strong fall off with increasing Q value. Therefore, further magnetization and EPR measurements would be more appropriate in elucidating the magnetic nature of $Li(NH_3)_4$ or $Li(ND_3)_4$. The present structure determinations of phase II and, in particular, phase III do enable band-structure and ab initio calculations to be undertaken along with a re-evaluation of the magnetism and electronic behavior; for example, possible coupling between small amplitude modulations of the itinerant electron spin density and the orientational changes of the fundamental tetrahedral complex building units of the structure.

The exploration and nature of conduction states in metal–ammonia systems has fascinated scientists for centuries. Last year marked the bi-centenary of the first observation[18] by Sir Humphry Davy of the striking blue and bronze colors of alkali–ammonia solutions and thus the inception of experimental observation and ongoing studies of solvated electrons.[19]

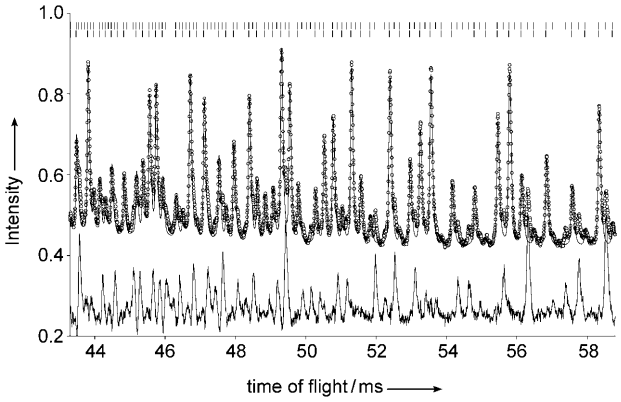

Figure 4. Section of a Pawley (intensity-only) fit to $Li(ND_3)_4$ at 10 K in space group $I\bar{4}3d$ showing observed (○), calculated (line), and difference (lower) profiles. The difference profile highlights the observation of supercell reflections, not fitted by this analysis, down to short d spacings (0.88–1.16 Å shown) and thus unlikely to result from magnetic scattering. Upper vertical bar markers indicate calculated Bragg peak positions in space group $P2_13$; lower markers correspond to $I\bar{4}3d$.

Experimental Section

2.5 g of $^7Li(ND_3)_4$ was prepared directly in thin-walled (0.25 mm) pure quartz (Supracil) ampoules, 10 mm diameter, 50 mm long, using sodium-dried ND_3 (Aldrich, 99%) and ^7Li (Oakridge, 99.95%) by standard vacuum techniques. The high-resolution neutron powder diffraction data used in the analysis were recorded on HRPD at the ISIS spallation neutron source Rutherford Appleton Laboratory, UK. The diffractometer has recently been upgraded with a new supermirror neutron guide allowing much improved data to be measured at high Q. Samples were loaded in a vanadium-tailed liquid-helium flow cryostat and neutron powder diffraction data measured rapidly (10 μAh, ca. 15 min) as a function of temperature between 4.2 K and just below the melting point at 85 K. Data of higher statistical quality (120 μAh, ca. 3 h) were subsequently measured at 10 K, 40 K, and 75 K to enable full structure refinement. Data were recorded over a time-of-flight range of 20–120 ms, corresponding to a d spacing range at backscattering ($< 2\theta \geq 168°$) of circa 0.4–2.4 Å. The instrumental resolution, $\Delta d/d$, is circa 8×10^{-4} and essentially constant as a function of d spacing.

Structure solution and refinement was carried out using the profile refinement program TOPAS-Academic.[20] The phase II structure at 40 K was refined using a starting model based on the previous neutron powder diffraction study by Young et al.[13] The

structure was refined without recourse to bond-length or bond-angle constraints and using common values for isotropic displacement parameters for both nitrogen atoms and all deuterium atoms in the asymmetric unit, respectively. The phase III structure at 10 K was solved in space group $P2_13$ requiring four unique $Li(ND_3)_4$ units in the asymmetric unit. A starting model was constructed using four $Li(ND_3)_4$ molecules defined as rigid bodies with idealized geometry and based on the 40 K refinement. The Li and N1 atoms on 16*c* sites in the phase II structure transform to individual 4*a* sites in the phase III structure arranged along the [111] direction. Initial constraints were applied to the molecular displacements from the starting bcc structure and these were determined using group theoretical methods implemented using the ISOTROPY software package.[21] The transformation is the result of a single irreducible representation—H1H2 following the notation of Stokes and Hatch.[21] For example, Li and N atoms on 4*a* sites have displacements and equal-sized anti-displacements associated with them along ⟨111⟩ and the remaining N and D atoms on general positions can be constrained using a further three separate displacements. Following initial convergence using this model the symmetry constraints were removed and then the rigid-body restraints were removed at the final stages of refinement. The final refinement agreement factors and crystallographic data are given in Table 1. A suitable starting point for structure refinement could also be obtained using simulated annealing methods implemented by TOPAS using rigid molecules constrained such that one Li–N bond of each molecule lies along ⟨111⟩. The crystal structures were visualized using the programs MERCURY[22] and DIAMOND.[23]

Crystallographic information (CIF) files can be obtained from the Inorganic Structural Database (ICSD). Further details on the crystal structure investigation(s) may be obtained from the Fachinformationszentrum Karlsruhe, 76344 Eggenstein-Leopoldshafen, Germany (fax: (+49) 7247-808-666; e-mail: crysdata@fiz-karlsruhe.de), on quoting the depository numbers 419839–419841 for the structures at 10, 40, and 75 K respectively. Figure showing results of the Rietveld fitting for $Li(ND_3)_4$-II at 40 K and 75 K and the crystal structure at 40 K are available as Supporting Information.

Received: September 2, 2008
Revised: November 11, 2008
Published online: January 15, 2009

Keywords: ammonia · lithium · neutron powder diffraction · structure elucidation

[1] J. C. Thompson, *Electrons in liquid ammonia*, Clarendon, Oxford, **1976**.
[2] N. Mammano in *Metal-ammonia solutions, Colloque Weyl II*, Butterworths, London, **1970**.
[3] W. S. Glaunsinger, R. B. Von Dreele, R. F. Marzke, R. C. Hanson, P. Chieux, P. Damay, R. Catterall, *J. Phys. Chem.* **1984**, *88*, 3860–3877.
[4] L. V. Coulter, J. K. Gibson, N. Mammano, *J. Phys. Chem.* **1984**, *88*, 3896–3900.
[5] E. W. LeMaster, J. C. Thompson, *J. Solid State Chem.* **1972**, *4*, 163–171.
[6] T. R. White, S. P. Hsu, M. J. Mobley, W. S. Glaunsinger, *J. Phys. Chem.* **1984**, *88*, 3890–3895.
[7] A. M. Stacy, D. C. Johnson, M. J. Sienko, *J. Chem. Phys.* **1982**, *76*, 4248–4254.
[8] A. M. Stacy, P. P. Edwards, M. J. Sienko, *J. Solid State Chem.* **1982**, *45*, 63–70.
[9] J. Kohanoff, F. Buda, M. Parrinello, M. L. Klein, *Phys. Rev. Lett.* **1994**, *73*, 3133–3136.
[10] A. M. Stacy, M. J. Sienko, *Inorg. Chem.* **1982**, *21*, 2294–2297.
[11] N. Mammano, M. J. Sienko, *J. Am. Chem. Soc.* **1968**, *90*, 6322.
[12] P. Chieux, M. J. Sienko, F. DeBaecker, *J. Phys. Chem.* **1975**, *79*, 2996–3000.
[13] V. G. Young, W. S. Glaunsinger, R. B. Von Dreele, *J. Am. Chem. Soc.* **1989**, *111*, 9260–9261.
[14] G. L. Martyna, M. L. Klein, *J. Phys. Chem.* **1991**, *95*, 515–518.
[15] J. L. Dye, M. J. Wagner, G. Overney, R. H. Huang, T. F. Nagy, D. Tomanek, *J. Am. Chem. Soc.* **1996**, *118*, 7329–7336.
[16] T. A. Kaplan, J. F. Harrison, J. L. Dye, R. Rencsok, *Phys. Rev. Lett.* **1995**, *75*, 978–978.
[17] M. H. Cohen, *Electrons in Fluids*, Springer, Heidelberg, **1973**.
[18] P. P. Edwards, *Adv. Inorg. Chem. Radiochem.* **1982**, *25*, 135–185.
[19] I.-R. Lee, W. Lee, A. H. Zewail, *ChemPhysChem* **2008**, *9*, 83–88.
[20] A. Coelho, http://members.optusnet.com.au/~alancoelho/, **2008**.
[21] H. T. Stokes, D. M. Hatch, B. J. Campbell, stokes.byu.edu/isotropy.html, **2007**.
[22] F. Macrae, P. R. Edgington, P. McCabe, E. Pidcock, G. P. Shields, R. Taylor, M. Towler, J. van de Streek, *J. Appl. Crystallogr.* **2006**, *39*, 453–457.
[23] C. Impact, Crystal Impact GbR, Bonn, Germany, **2004**.

